NK Cells Accumulate in Infected Tissues and Contribute to Pathogenicity of Ebola Virus in Mice

H. Fausther-Bovendo,[a,b]* X. Qiu,[a,b] S. He,[a,b] A. Bello,[a,b] J. Audet,[a,b] G. Ippolito,[c] G. Wong,[a,b]* ⬤ G. Kobinger[a,b,d]*

[a]National Microbiology Laboratory, Public Health Agency of Canada, Winnipeg, Canada
[b]University of Manitoba, Winnipeg, Canada
[c]National Institute for Infectious Diseases, Lazzaro Spallanzani, National Institute for Infectious Diseases–IRCCS, Rome, Italy
[d]Department of Pathology and Laboratory Medicine, University of Pennsylvania School of Medicine, Philadelphia, Pennsylvania, USA

ABSTRACT Understanding the immune parameters responsible for survival following Ebola virus (EBOV) infection is paramount for developing countermeasures. In lethal EBOV infections, levels of both NK and T cells decline drastically in the circulation and lymphoid tissues before death. However, the fate of these lymphocytes in viral replication sites remains unknown. In this study, reverse transcription-PCR (RT-PCR) and fluorescence-activated cell sorting (FACS) analysis were used to investigate lymphocyte frequencies in various infected mouse tissues after challenge with mouse-adapted EBOV (MA-EBOV). A decrease in NK cell numbers from systemic circulation was observed concomitant to an increase of these cells in tissues that are supporting active replication of EBOV. Unexpectedly, NK accumulation in virus replication sites correlated with enhanced EBOV disease progression in specific conditions; at a high challenge dose, NK-depleted mice displayed lower viremia and liver damage and higher hepatic T cell levels. Upregulation of UL16 binding protein 1 (ULBP-1) was detected in hepatic T cells, suggesting that NK cells participate in their elimination. Overall, this study supports the concept that NK cells accumulate in EBOV-infected tissues and can contribute to viral pathogenicity.

IMPORTANCE Ebola virus (EBOV) outbreaks can claim numerous lives and also devastate the local health infrastructure, as well as the economy, of affected countries. Lethal EBOV infection has been documented to decrease the levels of several immune cells in the blood that are necessary to defend the host. This decrease in immune cells is, however, not observed in individuals who survive EBOV infection. Having a better grasp of how these immune cells are lost is therefore of high importance to develop and improve new and existing therapeutics. The significance of our research is in identifying the mechanism responsible for the apparent loss of immune cells in lethal EBOV infection. This will allow therapeutic options aimed at preventing the loss of these immune cells, therefore allowing infected individuals to better fight the infection.

KEYWORDS Ebola virus, lymphopenia, NK cells, ULBP-1, autologous killing

Untreated Ebola virus (EBOV) infection can lead to a hemorrhagic fever and multiple organ failure followed by septic shock, leading to death in up to 90% of cases (1). During the 2014 to 2016 EBOV outbreak, the safety and efficacy of several therapeutic and prophylactic countermeasures were clinically evaluated (2). Although the protective efficacy of the vesicular stomatitis virus (VSV) vaccine was clinically demonstrated (3), statistically significant survival benefits are yet to be demonstrated by any therapeutic efficacy trials (4, 5). Understanding the immune properties specific to surviving or succumbing to an EBOV infection is important for the optimization of therapeutic products.

Lethal EBOV infections are characterized by an increase in granulocytes and a concomitant decrease in total lymphocyte counts in the systemic circulation. Among the lymphocyte populations, the relative frequencies of both T and NK cells drastically decline in the blood of infected individuals before death. A decrease in T cell levels was documented in human infections (6), while depletion of both T and NK cells was observed in nonhuman primates (NHPs) (7, 8) and rodents (9) infected with EBOV. Interestingly, this decrease was only observed in cases of lethal human infection but not in human survivors (6). This is of particular interest, as both NK and T cells are important players in EBOV clearance (10–12).

The mechanism responsible for the decline in circulating T and NK cells is suspected to be indirect, since neither T nor NK cells are infected by EBOV (7, 13). Apoptosis is currently believed to be one of the possible mechanisms responsible for the loss of T and NK cells. Numerous mechanisms, such as FAS/CD95- (6, 7, 14), TNF-related apoptosis-inducing ligand (TRAIL)- (7), and superantigen (15)-mediated cell death, have been proposed to explain T and NK cell apoptosis.

During EBOV infection, lymphocyte apoptosis has mainly been studied in peripheral blood and lymphoid tissues, including the spleen and lymph nodes of infected animals. (6–9, 16). However, the lymphopenia observed in peripheral blood and lymphoid tissues might not reflect the fate of lymphocyte populations in nonlymphoid tissues, such as the liver, lung, and kidney, where EBOV also replicates. T and NK cells migrate to infection sites in response to chemokine secretion. In addition, tissue-resident T and NK cell populations have been described in various nonlymphoid tissues, including the skin, liver, gut, uterus, and lungs (17, 18). Tissue-resident lymphocytes and their circulating counterparts often have distinct phenotypic and functional properties (19, 20), which could result in these pools of lymphocytes having different fates during an EBOV infection.

This study documents the fate of lymphocyte populations in various viral replication sites. This study also investigates the contribution of NK cell-mediated killing of immune cells to EBOV-induced lymphopenia. Here, both flow cytometry (fluorescence-activated cell sorting [FACS]) and reverse transcription-PCR (RT-PCR) were used to monitor the presence of NK cells in the blood and tissues of mice infected with mouse-adapted EBOV (MA-EBOV) when lymphopenia was detectable. Depletion studies of NK cells in mice were performed to investigate NK cell function during MA-EBOV infection. The level of activating NK ligands was also monitored in MA-EBOV-infected tissues to inform about putative bystander NK cell targets.

RESULTS

NK cells accumulate in viral replication sites during MA-EBOV infection. We sought to examine the fate of lymphocytes outside of the peripheral blood and lymphoid tissues during MA-EBOV infection. First, the kinetics of lymphopenia in peripheral blood were monitored in mice infected with a lethal dose of MA-EBOV (100 $\times$ 50% lethal dose [LD_{50}]). As previously reported, the total lymphocyte percentage started declining 3 days postinfection and remained low, around 30%. Similarly, total lymphocyte counts decreased from 3 days postchallenge but started rising 5 days postinfection (data not shown). Based on the above kinetics, the presence of T and NK cells was then monitored in subsequent experiments by RT-PCR and FACS in various tissues 4 days post MA-EBOV (100 $\times$ LD_{50}) challenge. The entire B cell population was used as a control, as its frequency within the lymphocyte population remains relatively stable during EBOV infection. Mice were either mock infected or infected with MA-EBOV. Four days postinfection, the spleen, kidney, lung, and liver were collected. The frequencies of T, NK, and B cells were first analyzed by RT-PCR. mRNA levels were normalized with actin to ensure that the loss of a specific immune subset would not artificially increase the frequency of other subsets. CD3Ɛ and CD19 mRNA levels decreased in all tissues assessed except for the liver and kidney, where no statistically significant changes in CD3Ɛ and CD19 mRNA levels were observed (Fig. 1), thus confirming the overall lymphopenia. In contrast, the NKp46 mRNA level decreased in
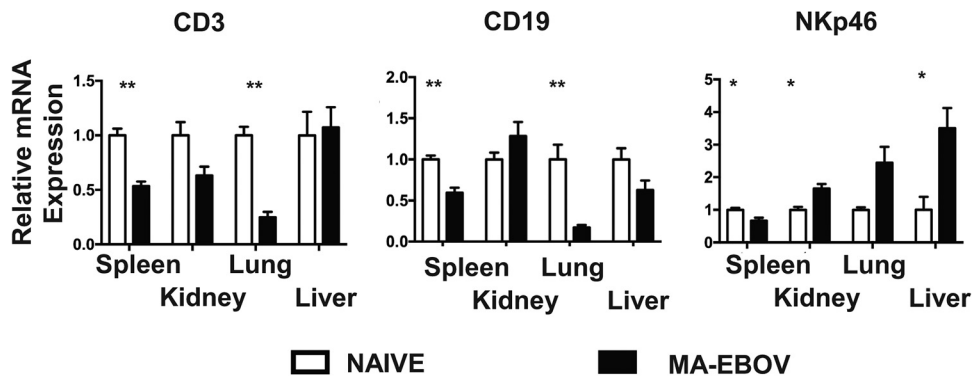
FIG 1 NK cell accumulation in MA-EBOV-infected tissues. Levels of CD3$\mathcal{E}$, CD19, and NKp46 mRNA were compared using RT-PCR of spleen, kidney, lungs, and liver from naive and MA-EBOV-infected ($100 \times LD_{50}$) mice 4 days after infection. Six mice were used per group, and actin was used to normalize mRNA for each sample. Relative mRNA expression levels (mean $\pm$ standard error of the mean [SEM]) are indicated.

the spleen of MA-EBOV-infected mice, while its level rose 1.7, 2.4, and 3.5-fold, respectively, in the kidney, lung, and liver of infected mice (Fig. 1), indicating an accumulation of NK cells to these organs at that time point. To further document the frequency of T, NK, and B cells *in vivo*, each respective population was measured by FACS in the above-mentioned tissues of MA-EBOV- and mock-infected mice. Within all tested tissues, there was no significant difference in the frequency of live hematopoietic cells (live CD45$^+$), which include both lymphocytes and granulocytes. As a result, frequencies of other immune subsets were expressed as the percentage of live CD45$^+$ cells. The frequencies of T and NK cells decreased, while the frequency of B cells slightly increased, in the spleen of MA-EBOV-infected mice. In the remaining MA-EBOV-infected tissues (liver, lungs, and kidney), there was a trend toward a lower B cell frequency and a sharp decline in T cell frequency. Conversely, in all these sites, the frequency of NK cells significantly increased, suggesting an NK cell accumulation within these tissues (Fig. 2). Taken together, both FACS and RT-PCR results suggest that NK, but not T, cells accumulate in MA-EBOV-infected tissues, also indirectly reinforcing previous studies indicating that T cell depletion is due to cell death.

Levels of IFN-α and KC, which modulate NK cell migration, are elevated after MA-EBOV infection. During hepatitis B virus (HBV) and murine cytomegalovirus (MCMV) infection, NK accumulation in the liver is dependent on interferon alpha (IFN-α) and IL-8 production (21, 22). To investigate a possible role of these cytokines in promoting NK cell accumulation in the liver during MA-EBOV replication, circulating levels of IFN-α, IL-8 and its murine homologue KC/CXCL1 (KC), and MIP2/CXCL2 (MIP2) (23) were measured by enzyme-linked immunosorbent assay (ELISA) 4 days postchallenge in mice. Elevated levels of IFN-α and KC, but not IL-8 or MIP2, were observed in sera from MA-EBOV-challenged mice (Fig. 3). These results suggest that elevated IFN-α and KC production could both contribute to NK cell accumulation in the liver during MA-EBOV infection.

The role of NK cells during EBOV infection is dependent on viral load. To better understand the role of NK cells during EBOV infection, NK depletion studies in BALB/c mice were performed using anti-asialo GM1 antibodies. NK-depleted mice were infected with either a low dose ($1 \times LD_{50}$) or a high dose ($100 \times LD_{50}$) of MA-EBOV. At low viral load, fewer NK-depleted mice survived the challenge compared with their mock-depleted counterparts (Fig. 4a). This suggests that NK cells can interfere with the progression of MA-EBOV-induced disease in these conditions. Interestingly, in mice infected with a 100-fold higher dose of MA-EBOV, no difference in survival rate was observed with or without NK cell depletion. However, NK-depleted mice had delayed times to symptom (weight loss) onset and death than the control mice, 7.6$\pm$ 0.2 days versus 5.8 $\pm$0.4 days, ($P < 0.001$) (Fig. 4b). Anti-asialo GM1 antibodies have been reported to deplete both NK and basophils (24). To ensure that the detrimental effect
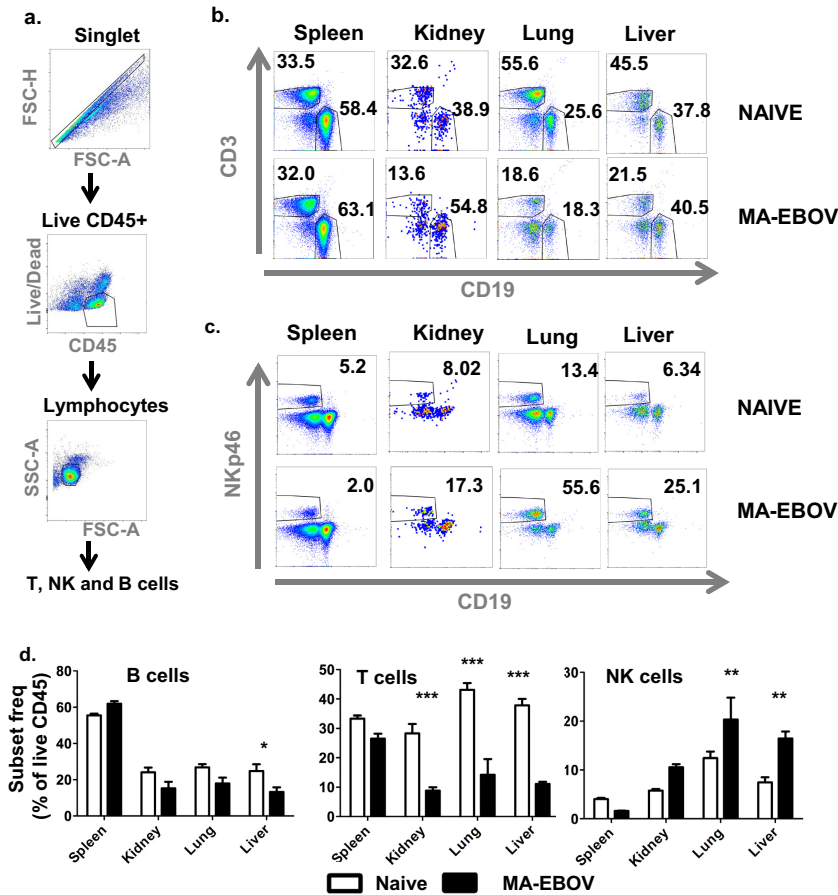
FIG 2 NK cell frequencies increased in MA-EBOV-infected tissues. Frequencies of live (live/dead low) B (CD45+ CD19+), T (CD45+ CD3+), and NK (CD45+ NKp46+) cells in spleen, kidney, lung, and liver were measured by FACS in naive and MA-EBOV-infected ($100 \times LD_{50}$) mice 4 days after infection. (a) Gating strategies for B, T, and NK cell frequencies. Representative plots of T, B (b), and NK cell (c) frequencies from the lymphocyte gate are illustrated. (d) Summary graphs ($n = 6$ per group) of B, T, and NK cell frequencies (mean ± SEM) are shown.

observed was due to NK cells, the latter challenge experiment was repeated in C57BL/6 mice using two distinct NK-depleting antibodies. Both anti-asialo GM1 and anti-NK1.1 delay the mean time to death of MA-EBOV-infected ($100 \times LD_{50}$) mice compare with mock-treated ones from 7.2 to 8.1 and 7.9 days postchallenge, respectively (Fig. 4c). This delayed time to death suggests that with higher initial viral load, the NK cell

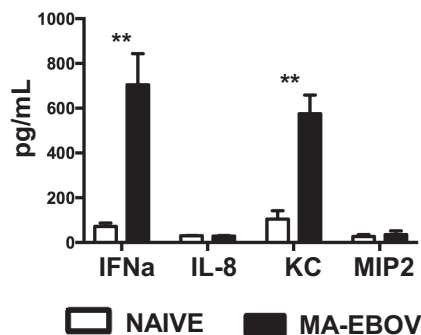**FIG 3** IFN-α and KC are induced after MA-EBOV challenge. Circulating level (mean ± SEM) of various cytokines were measured by ELISA in sera of naive (open bars) and MA-EBOV-infected ($100 \times LD_{50}$) mice (black bars) 4 days postchallenge. Results are representative of a single experiment with 8 mice per group.
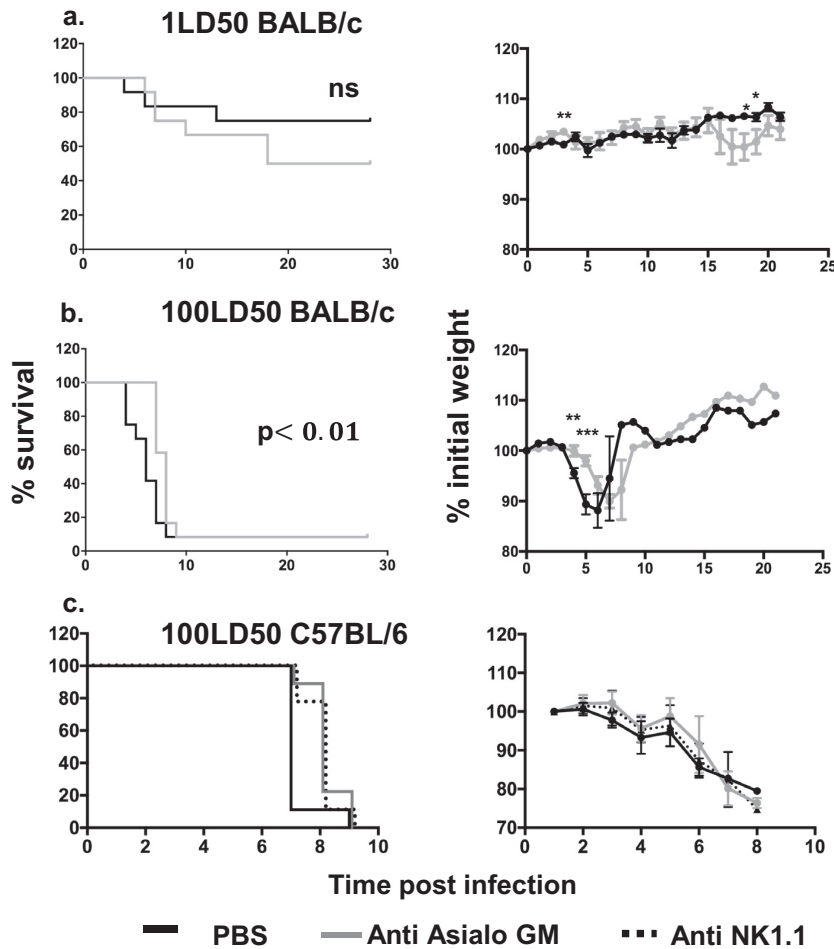
FIG 4 NK cells can have beneficial or detrimental roles depending on MA-EBOV infectious dose. BALB/c (a and b) and C57BL/6 mice (c) were treated with PBS (black lines) or one of two NK-depleting antibodies, anti-asialo GM1 (gray lines) or anti-NK1.1 (PK136) (dotted lines). Survival curves (left) and weight loss (right) are illustrated. (a and b) BALB/c mice ($n = 12$ per group) were infected with a low dose (1LD50) (a) or high dose (100LD50) of MA-EBOV (b) and monitored for 28 days postinfection. (c) C57BL/6 mice were infected with MA-EBOV (100LD50) and monitored postinfection. ns, non-statistically significant difference ($P > 0.05$).

response can be detrimental to the host. Interestingly, in the mouse model of lymphocytic choriomeningitis virus (LCMV) infection, NK cells differentially affect the host immune response, depending on the challenge dose (25).

NK depletion delays liver damage during MA-EBOV infection. To investigate the mechanism behind NK cell-mediated disease aggravation, viral load and liver damage were monitored in mock- and NK-depleted mice infected with MA-EBOV ($100 \times LD_{50}$). Based on elevated alanine aminotransferase (ALT) and alkaline phosphatase (ALP) levels, no significant liver damage was detectable 4 days post MA-EBOV challenge. As a result, the above parameters were assessed 5 days postchallenge. Viremia, ALP, and ALT levels were all greatly reduced (P values of 0.04, 0.02, and 0.05 respectively) in NK-depleted mice (Fig. 5a to c), further supporting the idea that NK cells can play a detrimental role in specific conditions related to Ebola virus replication.

Both T and B cells are involved in controlling viremia during EBOV infection (12, 26, 27). To probe the decreased viremia and liver damage in NK-depleted mice, hepatic levels of both T and B cells were compared by RT-PCR between mock- and NK-depleted mice infected with MA-EBOV. Although no difference in hepatic B cell level was detectable, there was on average a 1.56-fold increase in the hepatic T cell level in NK-depleted mice compared with that in their mock-depleted MA-EBOV-infected coun-
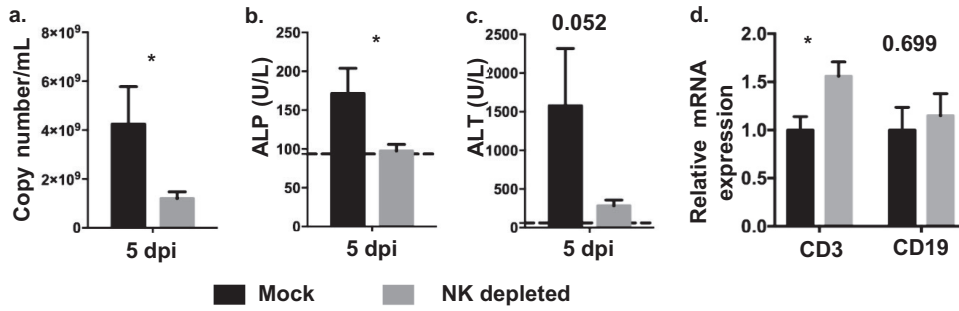
FIG 5 NK cells contribute to MA-EBOV pathogenicity. (a to c) Mock- (black) and NK-depleted mice (gray) were infected with a high dose ($100 \times LD_{50}$) of MA-EBOV. Five days postchallenge, viremia (a), ALP (b), and ALT (c) were measured by RT-PCR and using a VetScan VS2 instrument, respectively ($n = 8$ per group). Means ± SEM are shown; dotted lines represent the average values from naive mice ($n = 6$). (d) Levels of CD3ε and CD19 mRNA were compared by RT-PCR between mock- and NK-depleted mice challenged with MA-EBOV ($n = 6$ per group). Relative mRNA levels (mean ± SEM) are illustrated. *P* values are indicated where the differences fell short of statistical significance. NK depletion was achieved by injecting anti-asialo GM1 antibodies.

terpart (Fig. 5d). This result may indicate a direct or indirect pathogenic effect of NK cells toward hepatic T cells.

ULBP-1 is overexpressed by hematopoietic cells in the liver of MA-EBOV-infected mice. The phenomenon of NK cell-mediated pathogenicity was further investigated. We hypothesized that NK cell killing of hepatic T cells in MA-EBOV-infected mice was responsible for their detrimental effects at higher loads of MA-EBOV. Unfortunately, increased NK cell killing of hepatic T cells from MA-EBOV-infected mice could not be directly demonstrated using *in vitro* killing assays due to the limited number of lymphocytes which could be isolated from livers. Instead, expression of activating NK receptors and ligands was monitored on hepatic NK and T cells, respectively. Surface expression of activating TRAIL receptors or activating NKG2D ligands is sufficient for target cells to become sensitive to lysis by autologous NK cells expressing TRAIL or NKG2D, respectively. Levels of NKG2D and TRAIL were first monitored in hepatic NK cell by FACS in mock- or MA-EBOV-infected mice ($100 \times LD_{50}$). In MA-EBOV-infected mice, only 5% of NK cells in the liver expressed TRAIL on their surface (Fig. 6). In contrast, an average of 90% of NK cells expressed NKG2D in the liver of MA-EBOV-challenged mice (Fig. 6). Due to high level of NKG2D expression on NK cells, the amount of NKG2D ligands on T and B lymphocytes from the liver was measured in mock- or MA-EBOV-infected mice ($100 \times LD_{50}$). Of note, activating TRAIL receptors level were not measured on immune cells due to the low expression levels of TRAIL on NK cells. There was little

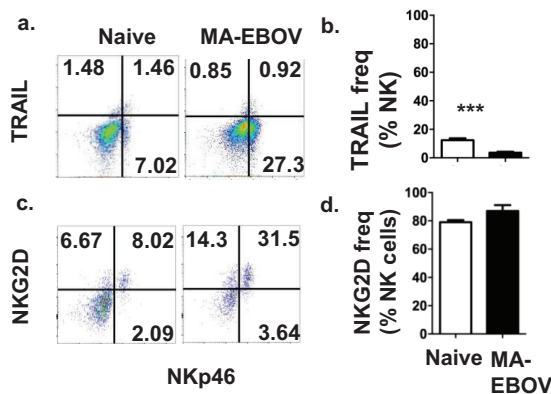**FIG 6** Abundant NKG2D but limited TRAIL expression was detected on liver NK cells from MA-EBOV-infected mice. On day 4 after MA-EBOV infection ($100 \times LD_{50}$), TRAIL (a and b) and NKG2D (c and d) surface expression on NK cells were measured by FACS, with naive mice used as negative controls. Representative (a and c) and summary graphs ($n = 6$/group; mean ±SEM) (b and d) are illustrated.
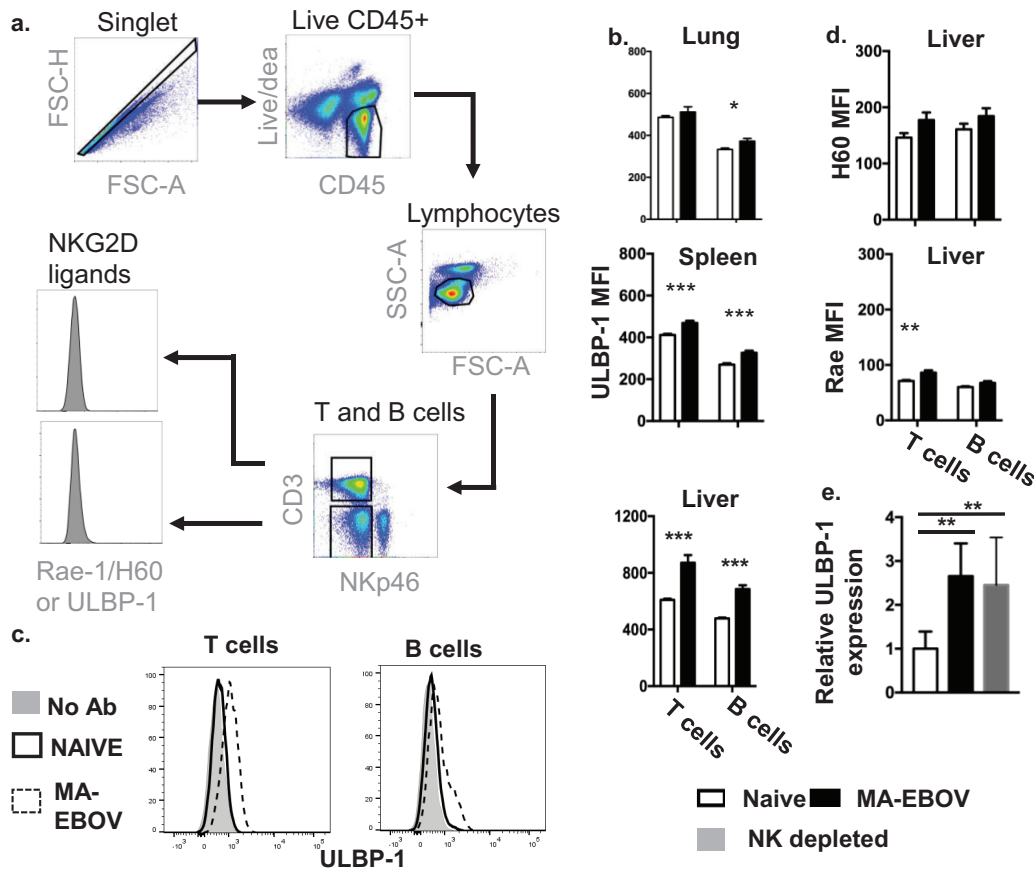
FIG 7 ULBP-1/MULT-1 is upregulated in the liver on MA-EBOV-infected mice. Levels of NKG2D ligands (ULBP-1, H60, and Rae-1) were measured by FACS on live T (live CD45$^+$ CD3$^+$ NKp46$^-$) and B cells (live CD45$^+$ CD3$^-$ NKp46$^-$) from spleen, lung, and liver of naive or MA-EBOV-infected mice (100 $\times$ LD$_{50}$) 4 days postchallenge. (n = 6/group). (a) Gating strategies for H60, Rae-1, and ULBP-1 expression levels. (b) ULBP-1 expression (mean $\pm$ SEM) on T and B cells from the spleen, lungs, and liver of mock- and MA-EBOV-infected mice are depicted. Summary graphs (b), as well as representative plots (c), are displayed for ULBP-1 (n = 9/group). (d) H60 and Rae-1 levels (mean $\pm$ SEM) on hepatic lymphocytes are illustrated. (e) Changes in ULBP-1 mRNA were also measured by RT-PCR between naive and MA-EBOV-infected mice (mock- or NK-depleted). Relative mRNA levels (mean $\pm$ SEM) are illustrated. NK depletion was achieved by injecting anti-asialo GM1 antibodies.

to no increase in the surface expression of H60 and Rae-1, two NKG2D-activating ligands, on T and B cells in the liver of infected mice compared to that in their naive counterparts. In contrast, surface expression of UL16 binding protein (ULBP-1), a third NKG2D-activating ligand, was significantly increased on the surface of T and B cells in the liver but not in other tested tissues from infected mice (Fig. 7a and d). To confirm the above FACS results, ULBP-1 mRNA levels were compared between naive and MA-EBOV-infected mice (100 $\times$ LD$_{50}$). Similar to the FACS results, there was a wide range of ULBP-1 induction levels in infected mice; overall, there was a 2.66-fold increase in ULBP-1 expression in the liver of MA-EBOV-infected mice compared with that in naive mice (Fig. 7e). It is worth pointing out that there was no difference in the ULBP-1 mRNA level between mock- and NK-depleted mice post MA-EBOV-challenge (Fig. 7e). ULBP-1 is probably induced by direct contact with MA-EBOV viral particles or by MA-EBOV-induced inflammation. Despite reduced NK killing of ULBP-1 cells, lower ULBP-1 induction in NK-depleted mice is probably responsible for the similar ULBP-1 expression levels of mock- and NK-depleted mice after MA-EBOV challenge.

ULBP-1 induction in T cells has previously been shown to render them sensitive to autologous NK cell-mediated killing (28). Therefore, the above results suggest that NK killing of ULBP-1-positive T cells in the liver may contribute to MA-EBOV immune evasion and viral pathogenicity.

DISCUSSION

NK cells possess multiple antiviral properties. They can kill infected cells, secrete inflammatory cytokines, and shape the adaptive response by interacting with dendritic cells (29–31). Accordingly, the beneficial impact of NK cells during MA-EBOV infection has previously been demonstrated in mice treated with virus-like particles (VLPs) or recombinant vesicular stomatitis virus encoding EBOV glycoprotein (VSV-GP) 1 to 3 days before or after challenge, respectively (11, 13).

The present study indicates that NK cell depletion in peripheral blood and the spleen of MA-EBOV-infected mice was concomitant with an accumulation of NK cells in nonlymphoid tissues. The sharpest increase in NK cell frequency was observed in the liver, which is a major replication site early after EBOV infection (7). This observation suggests that NK cell accumulation may directly correlate with viral load and EBOV-mediated inflammation. NK cells migrate in an IFN-α- and IL-8-dependent manner to the liver of HBV- and MCMV-infected individuals and mice, respectively (21, 22). MA-EBOV infection induces secretion of IFN-α and KC, the murine IL-8 homolog, suggesting that NK accumulation might results from circulating NK migration to replication sites. It is worth pointing out that proliferation of tissue-resident NK cells may also contribute to NK accumulation. Due to the lack of specific markers to differentiate tissue resident from circulating NK cells in our study, the contribution of each mechanism cannot be determined. Interestingly, a decrease in the number of circulating NK cells has also been described in NHPs infected with Lassa virus (32), suggesting that vast NK cell accumulation in sites of viral replication might be a common feature of viral hemorrhagic fevers.

Although the antiviral properties of NK cells are well documented, data obtained in this study indicate that the activity of NK cells can also be detrimental to the host. Infection of perforin-deficient mice previously suggested that killing of noninfected (bystander) cells may be involved in MA-EBOV disease aggravation (13). Here, NK depletion studies, in conjunction with the significant increase in ULBP-1 surface expression on T cells in the liver of MA-EBOV-infected mice, suggest NK cell killing of T cells. Although sufficient T and NK cells could not be obtained from liver to demonstrate *in vitro* NK killing of hepatic T cells from MA-EBOV-infected mice, Cerboni and colleagues (28) previously demonstrated NK killing of ULBP-1-positive T cells. Indeed, *in vitro* T cell activation leads to a similar increase in ULBP-1 surface expression, as well as an increase in susceptibility to autologous NK cells lysis via NKG2D (28). It is worth noting that NK killing of T lymphocytes within the liver of infected mice may contribute to MA-EBOV immune evasion. T cells are recruited to infection sites independently of antigen specificity (33, 34). Even though the role of these non-antigen-specific infiltrating cells is not fully understood, they are thought to participate in controlling invading pathogens by producing antiviral cytokines in response to the inflammatory cytokine milieu (35). Therefore, NK killing of T cells within the liver of infected mice, independently of their antigen specificity, may facilitate viral replication and therefore exacerbate liver damage, as MA-EBOV replication in hepatocytes leads to necrosis.

Additional mechanisms may also be involved in the observed NK cell-mediated MA-EBOV disease exacerbation. Indeed, no significant ULBP-1 induction on T cells was detected in the lungs of MA-EBOV-infected mice despite a reduction in pulmonary T cell frequency. In addition, MA-EBOV replicates heavily in the liver but not in the lungs of intraperitoneally challenged mice, resulting in substantially more immune activation, including cytokines in the liver. Taken together, the above observations suggest that distinct mechanisms in the lung versus the liver of MA-EBOV-infected mice could be at play.

NK killing of infected hepatocytes and epithelial cells could aggravate liver damage, while NK killing of infected antigen-presenting cells, such as dendritic cells and macrophages, might dampen the cellular response against MA-EBOV. In addition, T cell apoptosis due to improper activation rather than direct killing by NK cells may also be responsible for the decrease in T cell frequency in MA-EBOV-infected mice. Of note, 5

days post MA-EBOV infection, levels of virus-specific IgG are very low. As a result, NK-mediated antibody-dependent cellular cytotoxicity (ADCC) is not expected to contribute significantly to the disease aggravation observed in our experiments.

Together, our work suggests the following model, in which, after low MA-EBOV challenge dose, NK cells participate in viral clearance and therefore improve survival. In contrast, in untreated mice challenged with a high dose of MA-EBOV, NK cells contribute to viral pathogenicity. Treatments such as VLP or VSV-GP administration close to the time of challenge also promote a beneficial role of NK cells in mouse challenge with a high infectious dose by reducing the initial viral load (11, 13).

Data presented in this manuscript are restricted to the mouse model of EBOV infection and would therefore need confirmation in EBOV-infected individuals. However, data from EBOV-infected NHPs and individuals indicates that NK cell-mediated disease aggravation is probably not limited to the rodent model of EBOV infection. An increase in circulating IFN-α levels in NHPs challenged with a lethal dose of EBOV was previously reported (7). Wauquier and colleagues (36) also demonstrated that KIR2DS1 and KIR2DS3, two activating killer immunoglobulin-like receptors (KIR), which are expressed on NK cells and a subset of T cells, were more frequent in lethal EBOV infections than in EBOV survivors and the noninfected population. Whether additional NK-activating ligands, such as NKp44L and NKp30L, which do not have known murine equivalents (37), are also involved in disease aggravation in EBOV-infected individuals will require further investigation. It is worth noting that NK cell disease aggravation has been previously described in the context of other infections. In the mouse model of LCMV infection, viral challenge also induces expression of NKG2D ligands on T cells. Furthermore, NK depletion resulted in lower viremia, liver damage, and virus-specific T cell response (38). NK cells also exacerbate disease progression in Semliki Forest virus- (39) and *Streptococcus pneumonia* (40)-infected mice. In addition, NK cell killing of CD4 T cells has also been postulated to participate in the decline of CD4 T cells in HIV-1 infection (41, 42).

Overall, the evidence presented here supports the idea that the decrease in NK cell numbers from the systemic circulation is associated with an NK cell accumulation in nonlymphoid tissues supporting EBOV replication. This study also indicates that relocated NK cells can participate in MA-EBOV pathogenicity under specific conditions. Early reduction of initial viral load would influence the balance of NK cell-mediated functions and could led to better clinical management of infected individuals.

MATERIALS AND METHODS

Mice and virus strains. Five- to 6-week-old female BALB/c and C57BL/6 mice were purchased from Charles River (Quebec, Canada). Mice were infected with either $100 \times LD_{50}$ (high dose) or $1 \times LD_{50}$ (low dose) of mouse-adapted (MA) EBOV. The MA-EBOV strain used has been previously described (43) and is derived from the Mayinga strain of EBOV.

Antibodies. CD3 PE (500A2), NKp46 BV605 (29A1.4), CD19 PercPCy55 (1D3), CD45 alexa700 and CD45 APC-Cy7 (30-F11), CD8 PE-Cy7 (53-6.7), and CD4 BV605 (RM4-5) antibodies were purchased from BD Biosciences (San Jose, CA), while CD3-PeCy7 (17A2), NKP46-FITC (29A1.4), and TRAIL-PE (N2B2) were from BioLegend (San Diego, CA). The fixable viability dye eFluor 506 (eBioscience, San Diego, CA) or Live/Dead fixable far red dead cell stain kit (Life Technologies, Burlington, Canada) were used to exclude dead cells.

Flow cytometry. Spleen, lungs, liver, and kidneys from infected mice were harvested 4 days post MA-EBOV infection ($100 \times LD_{50}$). Corresponding tissues from healthy mice were used as a control. Tissues were homogenized using a plunger, and a single cell suspension was obtained after filtering the homogenate through a 22-μm cell strainer. After extensive washes with phosphate-buffered saline (PBS), samples were stained with the designated antibody cocktail and viability dye to exclude dead cells.

After staining, all samples were analyzed using an LSR II flow cytometer (BD Biosciences, San Jose, CA). Analysis was performed using Flow Jo software (TreeStar, Ashland, OR).

RT-PCR. Spleen, lungs, liver, and kidneys from naive or infected mice were harvested 4 days post mock or MA-EBOV infection ($100 \times LD_{50}$), respectively, and preserved in RNAlater (Qiagen, Toronto, Canada) until use. RNA was purified from 30 mg of each tissue using the RNeasy kit (Qiagen) according to the manufacturer's instructions. One μg of purified RNA was transcribed into cDNA using the High-Capacity RNA to cDNA kit (Life Technologies, Burlington, Canada) according to the manufacturer's instructions. Following reverse transcription (RT), 1 μl of cDNA was analyzed by PCR using the TaqMan gene expression master mix (Life Technologies) and with the following forward (F) and reverse (R)

primers and probes (P) in the 5′ to 3′ orientation; CD3Ɛ (F-GCCCAGAGGGCAAAACAAG; R-TGCGGATGG
GCTCATAGTCT; P-AGCGGCCACCACCTGTTCCCA), CD19 (F-CGCCAGGAGATTCTTCAAAGTG; R-AGAGCACA
TTCCCGTACTGGTT; P-CCTCCCTCGGGAAACGGGACC), and NKP46 (F-GACTCTCCCGAAACCCATCA; R-GTTC
ACCGAGTTTCCATTTGTG; P-TGGGCCAAACCCAGCATCATGG). The beta-actin (Mm01205647_g1) primer/
probes mix was from Life Technologies. PCR plates were run on a StepOnePlus thermocycler (Applied
Biosystems, Burlington, Canada). CD3Ɛ, CD19, and NKp46 mRNA levels were used to monitor T, B, and
NK cell frequencies, respectively, by RT-PCR, while beta-actin mRNA was used as a loading control. Fold
changes between tested mice were calculated based on the threshold cycle ($\Delta\Delta C_T$) method.

For ULBP-1 quantification, RT-PCR analysis was performed as described above, except ULBP-1
(Mm_ULBP1_1_SG) and actin-beta (Mn_Actb_1_SG) Quantitect primers were obtained from Qiagen, and
the PCRs were performed using the iQ SYBR green supermix (Bio-Rad, Mississauga, Canada) according to
the manufacturer's instructions.

NK depletion studies. For NK cell depletions, mice received either 40 μl of polyclonal rabbit
anti-asialo GM1 antibodies (Wako BioProducts, Richmond, VA) 1 day before MA-EBOV challenge and
on days 5, 11, and 18 postinfection or 100 μg of anti-mouse NK1.1 (PK136) antibodies (Cedarlane,
Burlington, Canada) 2 days before and on the day of challenge, as previously reported (44). Both
NK-depleted mice and control mice were monitored daily for survival, weight loss, and signs of
disease for 28 days after MA-EBOV infection. NK cell depletion efficiency was confirmed by FACS
using unchallenged mice.

Viremia. Mice were bled via the retro-orbital route into EDTA tubes (BD Biosciences, San Jose, CA).
Viremia was determined by RT-qPCR as previously reported (45). Briefly, RNA was extracted using QIAmp
Viral RNA mini kit (Qiagen). Levels of EBOV RNA polymerase were detected by RT-qPCR.

Blood counts and liver damage. Mice were bled via the retro-orbital route and sera were collected
using serum separation tubes (BD Biosciences). Blood counts were measured using a VetScan HM5
instrument (Abaxis Veterinary Diagnostics, Union City, CA), while alanine aminotransferase (ALT) and
alkaline phosphatase (ALP) levels were measured using a VetScan VS2 instrument (Abaxis Veterinary
Diagnostics).

Cytokine serum levels. IFN-α and IL-8 ELISA kits were purchased from eBioscience, Inc., and
MyBioSource, while KC and MIP2 ELISA kits were from Cedarlane. Serum levels were measured according
to the manufacturers' instructions.

Ethics statement. All infectious animal work was performed in the biosafety level 4 biocontainment
laboratory at the Public Health Agency of Canada. The procedures described in this manuscript were
approved under animal use document H13-009 by the Canadian Science Centre for Human and Animal
Health Care Committee, following the guidelines of the Canadian Council on Animal Care. Animals were
all acclimatized for at least 7 days prior to the start of any experiments. Animals were fed and monitored
daily before and during the course of the experiments.

Statistical analysis. Differences in immune cell frequencies were analyzed using a two-way ANOVA
test followed by a Bonferroni test, while differences in mRNA levels, NKG2D ligands, weight loss, cytokine
levels, ALT, ALP, and viremia were analyzed using unpaired t tests. For RT-PCR results, the mRNA level of
each sample was first normalized using actin (using the $\Delta\Delta C_T$ method), as previously described (46). All
statistical analyses were performed using GraphPad Prism version 5.03 software. Throughout this article,
*, **, and *** indicate statistically significant differences, with P values of <0.05, 0.01, and 0.001
respectively, while ns indicates a non-statistically significant difference ($P > 0.05$).

REFERENCES

1. Feldmann H, Geisbert TW. 2011. Ebola haemorrhagic fever. Lancet 377:
849–862. https://doi.org/10.1016/S0140-6736(10)60667-8.
2. Mendoza EJ, Qiu X, Kobinger GP. 2016. Progression of Ebola therapeutics
during the 2014–2015 outbreak. Trends Mol Med 22:164–173. https://
doi.org/10.1016/j.molmed.2015.12.005.
3. Henao-Restrepo AM, Longini IM, Egger M, Dean NE, Edmunds WJ, Ca-
macho A, Carroll MW, Doumbia M, Draguez B, Duraffour S, Enwere G,
Grais R, Gunther S, Hossmann S, Kondé MK, Kone S, Kuisma E, Levine
MM, Mandal S, Norheim G, Riveros X, Soumah A, Trelle S, Vicari AS,
Watson CH, Kéïta S, Kieny MP, Røttingen J-A. 2015. Efficacy and effec-
tiveness of an rVSV-vectored vaccine expressing Ebola surface
glycoprotein: interim results from the Guinea ring vaccination cluster-
randomised trial. Lancet 386:857–866. https://doi.org/10.1016/S0140
-6736(15)61117-5.
4. Davey RT, Dodd L, Proschan MA, Neaton J, Neuhaus Nordwall J,
Koopmeiners JS, Beigel J, Tierney J, Lane HC, Fauci AS, Massaquoi
MBF, Sahr F, Malvy D, PREVAIL II Writing Group, Multi-National PRE-
VAIL II Study Team. 2016. A randomized, controlled trial of ZMapp for
Ebola virus infection. N Engl J Med 375:1448–1456. https://doi.org/
10.1056/NEJMoa1604330.

5. Cardile AP, Downey LG, Wiseman PD, Warren TK, Bavari S. 2016. Antiviral therapeutics for the treatment of Ebola virus infection. Curr Opin Pharmacol 30:138–143. https://doi.org/10.1016/j.coph.2016.08.016.

6. Baize S, Leroy EM, Georges-Courbot MC, Capron M, Lansoud-Soukate J, Debré P, Fisher-Hoch SP, McCormick JB, Georges AJ. 1999. Defective humoral responses and extensive intravascular apoptosis are associated with fatal outcome in Ebola virus-infected patients. Nat Med 5:423–426. https://doi.org/10.1038/7422.

7. Geisbert TW, Hensley LE, Larsen T, Young HA, Reed DS, Geisbert JB, Scott DP, Kagan E, Jahrling PB, Davis KJ. 2003. Pathogenesis of Ebola hemorrhagic fever in cynomolgus macaques: evidence that dendritic cells are early and sustained targets of infection. Am J Pathol 163:2347–2370. https://doi.org/10.1016/S0002-9440(10)63591-2.

8. Reed DS, Hensley LE, Geisbert JB, Jahrling PB, Geisbert TW. 2004. Depletion of peripheral blood T lymphocytes and NK cells during the course of Ebola hemorrhagic fever in cynomolgus macaques. Viral Immunol 17:390–400. https://doi.org/10.1089/vim.2004.17.390.

9. Bradfute SB, Braun DR, Shamblin JD, Geisbert JB, Paragas J, Garrison A, Hensley LE, Geisbert TW. 2007. Lymphocyte death in a mouse model of Ebola virus infection. J Infect Dis 196:S296–S304. https://doi.org/10.1086/520602.

10. Gupta M, Mahanty S, Greer P, Towner JS, Shieh W-J, Zaki SR, Ahmed R, Rollin PE. 2004. Persistent infection with Ebola virus under conditions of partial immunity. J Virol 78:958–967. https://doi.org/10.1128/JVI.78.2.958-967.2004.

11. Warfield KL, Perkins JG, Swenson DL, Deal EM, Bosio CM, Aman MJ, Yokoyama WM, Young HA, Bavari S. 2004. Role of natural killer cells in innate protection against lethal Ebola virus infection. J Exp Med 200:169–179. https://doi.org/10.1084/jem.20032141.

12. Sullivan NJ, Hensley L, Asiedu C, Geisbert TW, Stanley D, Johnson J, Honko A, Olinger G, Bailey M, Geisbert JB, Reimann KA, Bao S, Rao S, Roederer M, Jahrling PB, Koup RA, Nabel GJ. 2011. CD8+ cellular immunity mediates rAd5 vaccine protection against Ebola virus infection of nonhuman primates. Nat Med 17:1128–1131. https://doi.org/10.1038/nm.2447.

13. Williams KJN, Qiu X, Fernando L, Jones SM, Alimonti JB. 2015. VSVΔG/EBOV GP-induced innate protection enhances natural killer cell activity to increase survival in a lethal mouse adapted Ebola virus infection. Viral Immunol 28:51–61. https://doi.org/10.1089/vim.2014.0069.

14. Wauquier N, Becquart P, Padilla C, Baize S, Leroy EM. 2010. Human fatal Zaire Ebola virus infection is associated with an aberrant innate immunity and with massive lymphocyte apoptosis. PLoS Negl Trop Dis 4:e837. https://doi.org/10.1371/journal.pntd.0000837.

15. Leroy EM, Becquart P, Wauquier N, Baize S. 2011. Evidence for Ebola virus superantigen activity. J Virol 85:4041–4042. https://doi.org/10.1128/JVI.00181-11.

16. Geisbert TW, Hensley LE, Gibb TR, Steele KE, Jaax NK, Jahrling PB. 2000. Apoptosis induced in vitro and in vivo during infection by Ebola and Marburg viruses. Lab Invest 80:171–186. https://doi.org/10.1038/labinvest.3780021.

17. Shi F-D, Ljunggren H-G, La Cava A, Van Kaer L. 2011. Organ-specific features of natural killer cells. Nat Rev Immunol 11:658–671. https://doi.org/10.1038/nri3065.

18. Lysakova-Devine T, O'Farrelly C. 2014. Tissue-specific NK cell populations and their origin. J Leukoc Biol 96:981–990. https://doi.org/10.1189/jlb.1RU0514-241R.

19. Park CO, Kupper TS. 2015. The emerging role of resident memory T cells in protective immunity and inflammatory disease. Nat Med 21:688–697. https://doi.org/10.1038/nm.3883.

20. Fan X, Rudensky AY. 2016. Hallmarks of tissue-resident lymphocytes. Cell 164:1198–1211. https://doi.org/10.1016/j.cell.2016.02.048.

21. Dunn C, Brunetto M, Reynolds G, Christophides T, Kennedy PT, Lampertico P, Das A, Lopes AR, Borrow P, Williams K, Humphreys E, Afford S, Adams DH, Bertoletti A, Maini MK. 2007. Cytokines induced during chronic hepatitis B virus infection promote a pathway for NK cell-mediated liver damage. J Exp Med 204:667–680. https://doi.org/10.1084/jem.20061287.

22. Salazar-Mather TP, Lewis CA, Biron CA. 2002. Type I interferons regulate inflammatory cell trafficking and macrophage inflammatory protein 1alpha delivery to the liver. J Clin Invest 110:321–330. https://doi.org/10.1172/JCI0215376.

23. Bozic CR, Gerard NP, von Uexkull-Guldenband C, Kolakowski LF, Conklyn MJ, Breslow R, Showell HJ, Gerard C. 1994. The murine interleukin 8 type B receptor homologue and its ligands. Expression and biological characterization. J Biol Chem 269:29355–29358.

24. Nishikado H, Mukai K, Kawano Y, Minegishi Y, Karasuyama H. 2011. NK cell-depleting anti-asialo GM1 antibody exhibits a lethal off-target effect on basophils in vivo. J Immunol 186:5766–5771. https://doi.org/10.4049/jimmunol.1100370.

25. Waggoner SN, Cornberg M, Selin LK, Welsh RM. 2012. Natural killer cells act as rheostats modulating antiviral T cells. Nature 481:394–398. https://doi.org/10.1038/nature10624.

26. Wong G, Richardson JS, Pillet S, Patel A, Qiu X, Alimonti J, Hogan J, Zhang Y, Takada A, Feldmann H, Kobinger GP. 2012. Immune parameters correlate with protection against Ebola virus infection in rodents and nonhuman primates. Sci Transl Med 4:158ra146. https://doi.org/10.1126/scitranslmed.3004582.

27. Marzi A, Engelmann F, Feldmann F, Haberthur K, Shupert WL, Brining D, Scott DP, Geisbert TW, Kawaoka Y, Katze MG, Feldmann H, Messaoudi I. 2013. Antibodies are necessary for rVSV/ZEBOV-GP-mediated protection against lethal Ebola virus challenge in nonhuman primates. Proc Natl Acad Sci U S A 110:1893–1898. https://doi.org/10.1073/pnas.1209591110.

28. Cerboni C, Zingoni A, Cippitelli M, Piccoli M, Frati L, Santoni A. 2007. Antigen-activated human T lymphocytes express cell-surface NKG2D ligands via an ATM/ATR-dependent mechanism and become susceptible to autologous NK⁻ cell lysis. Blood 110:606–615. https://doi.org/10.1182/blood-2006-10-052720.

29. Moretta A, Marcenaro E, Parolini S, Ferlazzo G, Moretta L. 2008. NK cells at the interface between innate and adaptive immunity. Cell Death Differ 15:226–233. https://doi.org/10.1038/sj.cdd.4402170.

30. Ferlazzo G, Münz C. 2009. Dendritic cell interactions with NK cells from different tissues. J Clin Immunol 29:265–273. https://doi.org/10.1007/s10875-009-9283-y.

31. Wehner R, Dietze K, Bachmann M, Schmitz M. 2011. The bidirectional crosstalk between human dendritic cells and natural killer cells. J Innate Immun 3:258–263. https://doi.org/10.1159/000323923.

32. Baize S, Marianneau P, Loth P, Reynard S, Journeaux A, Chevallier M, Tordo N, Deubel V, Contamin H. 2009. Early and strong immune responses are associated with control of viral replication and recovery in Lassa virus-infected cynomolgus monkeys. J Virol 83:5890–5903. https://doi.org/10.1128/JVI.01948-08.

33. Ely KH, Cauley LS, Roberts AD, Brennan JW, Cookenham T, Woodland DL. 2003. Nonspecific recruitment of memory CD8+ T cells to the lung airways during respiratory virus infections. J Immunol 170:1423–1429. https://doi.org/10.4049/jimmunol.170.3.1423.

34. Chen AM, Khanna N, Stohlman SA, Bergmann CC. 2005. Virus-specific and bystander CD8 T cells recruited during virus-induced encephalomyelitis. J Virol 79:4700–4708. https://doi.org/10.1128/JVI.79.8.4700-4708.2005.

35. Berg RE, Forman J. 2006. The role of CD8 T cells in innate immunity and in antigen non-specific protection. Curr Opin Immunol 18:338–343. https://doi.org/10.1016/j.coi.2006.03.010.

36. Wauquier N, Padilla C, Becquart P, Leroy E, Vieillard V. 2010. Association of KIR2DS1 and KIR2DS3 with fatal outcome in Ebola virus infection. Immunogenetics 62:767–771. https://doi.org/10.1007/s00251-010-0480-x.

37. Lanier LL. 2008. Up on the tightrope: natural killer cell activation and inhibition. Nat Immunol 9:495–502. https://doi.org/10.1038/ni1581.

38. Lang PA, Lang KS, Xu HC, Grusdat M, Parish IA, Recher M, Elford AR, Dhanji S, Shaabani N, Tran CW, Dissanayake D, Rahbar R, Ghazarian M, Brüstle A, Fine J, Chen P, Weaver CT, Klose C, Diefenbach A, Häussinger D, Carlyle JR, Kaech SM, Mak TW, Ohashi PS. 2012. Natural killer cell activation enhances immune pathology and promotes chronic infection by limiting CD8+ T-cell immunity. Proc Natl Acad Sci U S A 109:1210–1215. https://doi.org/10.1073/pnas.1118834109.

39. Alsharifi M, Lobigs M, Simon MM, Kersten A, Müller K, Koskinen A, Lee E, Müllbacher A. 2006. NK cell-mediated immunopathology during an acute viral infection of the CNS. Eur J Immunol 36:887–896. https://doi.org/10.1002/eji.200535342.

40. Kerr AR, Kirkham LAS, Kadioglu A, Andrew PW, Garside P, Thompson H, Mitchell TJ. 2005. Identification of a detrimental role for NK cells in pneumococcal pneumonia and sepsis in immunocompromised hosts. Microbes Infect 7:845–852. https://doi.org/10.1016/j.micinf.2005.02.011.

41. Vieillard V, Strominger JL, Debré P. 2005. NK cytotoxicity against CD4+ T cells during HIV-1 infection: a gp41 peptide induces the expression of an NKp44 ligand. Proc Natl Acad Sci U S A 102:10981–10986. https://doi.org/10.1073/pnas.0504315102.

42. Vieillard V, Dereuddre-Bosquet N, Mangeot-Méderlé I, Le Grand R, Debré P. 2012. An HIVgp41 vaccine protects CD4 central memory T cells in SHIV-infected macaques. Vaccine 30:6883–6891. https://doi.org/10.1016/j.vaccine.2012.09.004.

43. Bray M, Davis K, Geisbert T, Schmaljohn C, Huggins J. 1998. A mouse model for evaluation of prophylaxis and therapy of Ebola hemorrhagic fever. J Infect Dis 178:651–661. https://doi.org/10.1086/515386.

44. Smyth MJ, Thia KY, Street SE, Cretney E, Trapani JA, Taniguchi M, Kawano T, Pelikan SB, Crowe NY, Godfrey DI. 2000. Differential tumor surveillance by natural killer (NK) and NKT cells. J Exp Med 191:661–668. https://doi.org/10.1084/jem.191.4.661.

45. Qiu X, Wong G, Audet J, Bello A, Fernando L, Alimonti JB, Fausther-Bovendo H, Wei H, Aviles J, Hiatt E, Johnson A, Morton J, Swope K, Bohorov O, Bohorova N, Goodman C, Kim D, Pauly MH, Velasco J, Pettitt J, Olinger GG, Whaley K, Xu B, Strong JE, Zeitlin L, Kobinger GP. 2014. Reversion of advanced Ebola virus disease in nonhuman primates with ZMapp. Nature 514:47–53. https://doi.org/10.1038/nature13777.

46. Schmittgen TD, Livak KJ. 2008. Analyzing real-time PCR data by the comparative C_T method. Nat Protoc 3:1101–1108. https://doi.org/10.1038/nprot.2008.73.